BMC Plant Biology

RESEARCH Open Access

Multi-omics analyses reveal the mechanisms underlying the responses of *Casuarina equisetifolia* ssp. *incana* to seawater atomization and encroachment stress

Shike Zhang[1,2], Guobing Wang[2], Weiwei Yu[2], Long Wei[3], Chao Gao[2], Di Li[2], Lili Guo[2], Jianbo Yang[2], Shuguang Jian[1*] and Nan Liu[1*]

Abstract

Casuarina equisetifolia trees are used as windbreaks in subtropical and tropical coastal zones, while *C. equisetifolia* windbreak forests can be degraded by seawater atomization (SA) and seawater encroachment (SE). To investigate the mechanisms underlying the response of *C. equisetifolia* to SA and SE stress, the transcriptome and metabolome of *C. equisetifolia* seedlings treated with control, SA, and SE treatments were analyzed. We identified 737, 3232, 3138, and 3899 differentially expressed genes (SA and SE for 2 and 24 h), and 46, 66, 62, and 65 differentially accumulated metabolites (SA and SE for 12 and 24 h). The Kyoto Encyclopedia of Genes and Genomes (KEGG) enrichment analysis showed that SA and SE stress significantly altered the expression of genes related to plant hormone signal transduction, plant–pathogen interaction, and starch and sucrose metabolism pathways. The accumulation of metabolites associated with the biosynthetic pathways of phenylpropanoid and amino acids, as well as starch and sucrose metabolism, and glycolysis/gluconeogenesis were significantly altered in *C. equisetifolia* subjected to SA and SE stress. In conclusion, *C. equisetifolia* responds to SA and SE stress by regulating plant hormone signal transduction, plant–pathogen interaction, biosynthesis of phenylpropanoid and amino acids, starch and sucrose metabolism, and glycolysis/gluconeogenesis pathways. Compared with SA stress, *C. equisetifolia* had a stronger perception and response to SE stress, which required more genes and metabolites to be regulated. This study enhances our understandings of how *C. equisetifolia* responds to two types of seawater stresses at transcriptional and metabolic levels. It also offers a theoretical framework for effective coastal vegetation management in tropical and subtropical regions.

Keywords *Casuarina equisetifolia*, Transcriptome, Metabolome, Seawater atomization, Seawater encroachment

*Correspondence:
Shuguang Jian
jiansg@scbg.ac.cn
Nan Liu
liunan@scbg.ac.cn
[1]Guangdong Provincial Key Laboratory of Applied Botany, South China Botanical Garden, Chinese Academy of Sciences, Guangzhou 510650, China
[2]Institute of Geographical Sciences, Henan Academy of Sciences, Zhengzhou 450052, China
[3]Guangdong Provincial Key Laboratory of Silviculture, Protection and Utilization, Guangdong Coastal Shelterbelt Ecosystem National Observation and Research Station, Guangdong Academy of Forestry, Guangzhou 510520, China

Introduction

Plants, as sessile organisms, are often subjected to environmental stress such as drought, cold, heat, and salinity [1]. Salinity stress diminishes soil fertility and precipitates soil degradation, adversely impacting plant growth by hindering water and nutrient uptake [2]. Notably, the worldwide terrestrial zone characterized by elevated salinity surpasses 900 million hectares and continues to expand as a result of climate change and anthropogenic influences [3, 4]. Unraveling the mechanisms underlying plant responses to saline stress can enhance the efficiency of utilizing highly saline soils [4].

The ability to withstand high salinity is crucial for flora in coastal ecosystems. The current study focuses on the impact of salt stress on *Casuarina equisetifolia*, a species indigenous to Australia and the Pacific Islands. *C. equisetifolia* is characterized by rapid growth and the capacity to endure extreme drought, intense light, and elevated salinity, making it vital for windbreaks and sand stabilization in the southeastern coastal regions of Asia and tropical zones of the Americas [5]. Despite its remarkable resilience to saline conditions, including resistance to seawater atomization (SA) and seawater encroachment (SE) caused by typhoons [6–8], the underlying molecular mechanisms about this tolerance remain unclear.

Omics provides a comprehensive approach to elucidating the molecular mechanisms underlying plant responses to saline stress at the genomic, proteomic, and metabolomic levels [9]. Salt stress influences the expression of particular genes, as well as the accumulation of proteins and metabolites within both primary and secondary metabolic pathways in plants [1, 10–12]. Under salt stress, plants regulate osmotic pressure through the accumulation of amino acids and the expression of related genes[2, 4]. Transcriptomic analysis of Chinese cabbage (*Brassica rapa*) under salt stress indicated that differentially expressed genes (DEGs) were predominantly associated with amino acid biosynthesis and carbon metabolism [4]. Additionally, comparative metabolomic profiling of *Salvadora persica* revealed that heightened salinity levels led to an increased accumulation of glutamate, glycine, and cysteine [2]. Besides amino acids, starch and soluble sugars play a significant role in enhancing plant salt tolerance [13]. Transcriptomic and proteomic analyses of *Thellungiella halophila* identified that the proteins and genes related to starch and sucrose metabolism are essential for sustaining salt tolerance [14]. Furthermore, studies have demonstrated that plants have developed mechanisms to synthesize secondary metabolites, such as phenylpropanoids and flavonoids, as a response to salt stress [1]. Within the phenylpropanoid biosynthesis pathway, numerous substrates are involved in the production of flavonoids, phenols, and lignin, which are crucial for plant adaptation to environmental stress [12, 15]. As scavengers of reactive oxygen species (ROS), phenols mitigate the impact of oxidative stress, while lignin helps preserve the structural integrity of the xylem during salt exposure [4, 12]. Moreover, comparative analyses of transcriptomes, proteomes, and metabolomes in Chinese cabbage and cotton subjected to salt stress showed that genes encoding enzymes in the phenylpropanoid biosynthesis pathway were upregulated, leading to enhanced accumulation of phenols, flavonoids, and lignin [4, 12, 16].

Plants modulate the expression of genes associated with salt stress through a multitude of signaling pathways, notably incorporating hormone signal transduction pathways, the ROS signaling pathway, and the mitogen-activated protein kinase (MAPK) cascade [17, 18]. Additionally, plant hormone signaling pathways play a pivotal role in enhancing salt tolerance, with the abscisic acid (ABA) signaling pathway serving as the central mechanism [19, 20]. Transcriptomic and proteomic analyses of Chinese cabbage and foxtail millet (*Setaria italica*) showed that the ABA signaling pathway transmitted the signal of salt stress downstream to regulate gene expression [4, 21]. Importantly, salt stress prompts plants to generate ROS, which function as an indirect signal that activates various signaling pathways, including the MAPK cascade [22]. The activated pathways mitigate ROS toxicity by regulating Na^+ and K^+ transport to improve salt tolerance [23].

Researchers have evaluated the alterations in transcription factors (TFs), genes, osmotic substances (such as proline), and ions (specifically Na^+ and K^+) that contribute to the salt stress tolerance of *C. equisetifolia* to salt stress, but previous studies have predominantly concentrated on physiological and transcriptional adaptations to NaCl treatment [5, 24–28]. Furthermore, the impacts of two types of salt stress (SA and SE) that contribute to the degradation of *C. equisetifolia* windbreak forests have not been examined. In this study, we performed simulations of SA by atomizing a NaCl solution and SE by flooding with a NaCl solution to elucidate the underlying mechanisms of *C. equisetifoli*a responses to salt stress. We expected that the results would increase our understanding of the response mechanisms of *C. equisetifolia* to SA and SE stress, while also providing a theoretical foundation for efficient coastal vegetation management.

Materials and methods

Plant materials and salt treatments

The *C. equisetifolia* ssp. *incana* seedlings used in this study were germinated from seeds, and they were 20 cm tall when transplanted into pots. Each pot had an internal diameter and height of 17.5 cm, accommodating three seedlings per pot. The growth medium consisted of a substrate blend of sand and coconut coir (3:1, v/v).

To eliminate potential effects of mycorrhizae or nodules, the substrate components were sterilized using gamma radiation. The pots containing the seedlings were randomly arranged within the greenhouse of the South China Botanical Garden, Chinese Academy of Sciences (Guangzhou, Guangdong Province, China). The arrangement of pots was systematically altered to guarantee that the seedlings experienced minimal interference from light and moisture. The experimental design incorporated three treatments, namely, a control treatment (CT), SA, and SE. Each pot in both the CT and SA groups received 50 mL of water daily. For the SA group, the seedlings were positioned within a nearly sealed chamber constructed of a metallic framework and transparent plastic film (Fig. S1a), equipped with a humidifier. The humidifier atomized a 33‰ NaCl solution, mimicking the salinity levels of the surface seawater in the South China Sea [29]. The seedlings within the SE group were fully submerged in the same NaCl solution (Fig. S1b). The young branchlets from the seedlings across the SA, SE, and CT groups were harvested at 0, 2, 12, and 24 h post-treatment for transcriptomic analysis (at 0, 2, and 24 h) and metabolomic studies (at 0, 12, and 24 h). For each treatment, ten seeding pots (thirty seedlings) with similar seedling growth status were selected to collect sample. The young branches from ten seedlings were harvested to serve as a biological replicate, with three such biological replicates conducted. All seedlings were treated and harvested at the same time of day to exclude the effects of rhythm on gene expression and metabolite synthesis. Upon collection, the plant samples were wrapped in aluminum foil, frozen in liquid nitrogen, and stored at −80 °C for subsequent analysis.

RNA extraction, transcriptome sequencing, and analysis

The total RNA from each branchlet sample was extracted using Trizol reagent (Invitrogen, Waltham, USA). The determination of the integrity and the purification of RNA, library construction, and sequencing were conducted by Shanghai Majorbio Bio-pharm Biotechnology Co., Ltd. (Majorbio, Shanghai, China) using the Illumina NovaSeq 6000 sequencer (Illumina, California, USA). Subsequently, the clean reads were aligned to the *C. equisetifolia* genome [30] using HISAT2 [31]. The expression level of each gene was calculated according to transcripts per million fragments (FPKM) by RSEM [32]. Genes with $|\log_2(\text{fold change})| \geq 2.0$ and *P*-adjusted < 0.05 by DESeq2 were considered to be DEGs [33]. Additionally, KEGG (Kyoto Encyclopedia of Genes and Genomes, www.genome.jp/kegg) enrichment analysis was used to determine the metabolic pathways in which DEGs were significantly enriched at the *P*-adjusted < 0.05 level using KOBAS (http://kobas.cbi.pku.edu.cn/home.do) [34]. The sequenced raw reads generated in this study have been submitted to NCBI with BioProject ID: PRJNA983994 (https://dataview.ncbi.nlm.nih.gov/object/PRJNA983994?reviewer=9l7862c0ce35e9ad0jrtt8t87b).

Widely targeted metabolomics analysis

The extraction and analysis of the metabolome were performed by Metware Biotechnology Co., Ltd. (Metware, Wuhan, China). After the lyophilized sample was ground in a MM 400 mixer (Retsch, Düsseldorf, Germany), 100 mg of powder was added to 0.6 ml of 70% methanol. The sample was then placed at 4 °C overnight and was centrifuged at 10,000 × g for 10 min before the supernatant was passed through a microporous filter membrane (0.22-μm pore size). The filtrate was analyzed using a UPLC-MS/MS system composed of UPLC (Shimpack UFLC SHIMADZU CBM30A, Shimadzu, Japan) and MS / MS (4500 QTRAP, Applied Biosystems, USA). The working conditions of UPLC and MS were set as detailed prior [35]. The qualitative analysis of metabolites was performed utilizing the Metware database (MWDB) of Metware Biotechnology Co., Ltd. Metabolites were considered to be differentially accumulated metabolites (DAMs) when the variable importance in projection (VIP) was ≥ 1 and the absolute $\log_2$ (fold change) was ≥ 1.

Quantitative real-time polymerase chain reaction

The cDNAs from each group of samples (CT, SA_2h, SA_24h, SE_2h, and SE_24h) were used for quantitative real-time polymerase chain reaction (qRT-PCR). The cDNAs were synthesized from RNA according to the instructions of a GoScript™ Reverse Transcription System (Promega, USA). The qRT-PCR was carried out in a LightCycler® 480 II real-time PCR system (Roche, Switzerland) utilizing Unique Aptamer™ qPCR SYBR® Green Master Mix (Novogene, China). The PCR cycling parameters were 95 °C for 120 s, 40 cycles of 95 °C for 15 s, 60 °C for 60 s, 95 °C for 15 s, 60 °C for 60 s, 95 °C for 15 s, and 60 °C for 15 s [36]. The *elongation factor 1-alpha* (*EF1α*) and *ubiquitin* (*UBI*) were used as reference genes [25, 37]. The expression level of a target gene was calculated based on the $2^{-\Delta\Delta CT}$ method [38]. The expression levels of genes in all of the samples (CT, SA_2h, SA_24h, SE_2h, and SE_24h) were set to 1 in CT, and there were three biological and technical replicates. The primers for qRT-PCR were designed by Integrated DNA Technologies (http://www.idtdna.com/Primerquest/Home); these are listed in Table S1.

Results

Genes in response to SA and SE stress

To assess the transcriptional response of *C. equisetifolia* to SA and SE, we conducted Illumina high-throughput sequencing on branchlets subjected to CT, SA, or SE treatments. A total of 250,684,171 clean reads were

obtained from the five groups of samples (CT, SA_2h, SA_24h, SE_2h, and SE_24h), with the Q30% ranging from 95.05 to 95.32%, and the GC content ranging from 47.54 to 47.92%. According to the reference database, the total mapping percentage was greater than 92.38%, and over 86.83% of the clean reads could be uniquely mapped in every group of samples (Table S2).

We found that a total of 11,006 DEGs were involved in the responses to SA and SE stress. Compared with the CT group, we identified 737 DEGs (492 up and 245 downregulated), 3232 DEGs (2077 up and 1155 downregulated), 3138 DEGs (1482 up and 1656 downregulated), and 3899 DEGs (1901 up and 1998 downregulated) in group comparisons SA_2h/CT, SA_24h/CT, SE_2h/CT, and SE_24h/CT, respectively (Fig. 1a). A Venn diagram demonstrated that 218 DEGs were shared across the four sample groups, indicating their involvement in the response to both SA and SE treatments (Fig. 1b). Hierarchical cluster analysis conducted on common DEGs identified six clusters (Fig. 1c) and elucidated four different expression patterns within these clusters. Following treatments with SA and SE, the expression levels of genes in clusters 3, 2, and 4 exhibited upregulation, whereas cluster 1 demonstrated a downregulation in gene expression. Notably, gene expression levels in cluster 5 were elevated under SA treatment but showed a downregulation under SE treatment, with the expression pattern in cluster 6 displaying an inverse trend compared to that of cluster 5 (Fig. S2).

The KEGG pathway enrichment analysis was used to elucidate the biological functions of the common DEGs. The results indicated that the genes within clusters 1, 2, and 3 exhibited significant enrichment in pathways including phenylpropanoid biosynthesis pathway, thiamine metabolism, flavonoid biosynthesis, plant–pathogen interaction, amino sugar and nucleotide sugar metabolism, and the glycolysis/gluconeogenesis pathways (Fig. 1d). All DEGs from SA_2h/CT, SA_24h/CT, SE_2h/CT, and SE_24h/CT were subjected to KEGG pathway enrichment analysis. Notably, among the top five pathways with the highest DEG counts for both SA_2h/CT and SA_24h/CT, four were consistent, namely phenylpropanoid biosynthesis, plant–pathogen interaction, flavonoid biosynthesis, and the MAPK signaling pathway (Fig. S3). In SE_2h/CT and SE_24h/CT, the top five pathways with the most DEGs were shared, which included plant hormone signal transduction, phenylpropanoid biosynthesis, starch and sucrose metabolism, plant–pathogen interaction, and the MAPK signaling pathway (Fig. S4). Furthermore, an increase in the duration of SA or SE treatments correlated with a rise in the number of DEGs within the same pathways (Table S3).

To verify the accuracy of transcriptome data with SA and SE treatments, four DEGs from the phenylpropanoid biosynthesis and plant–pathogen interaction pathways

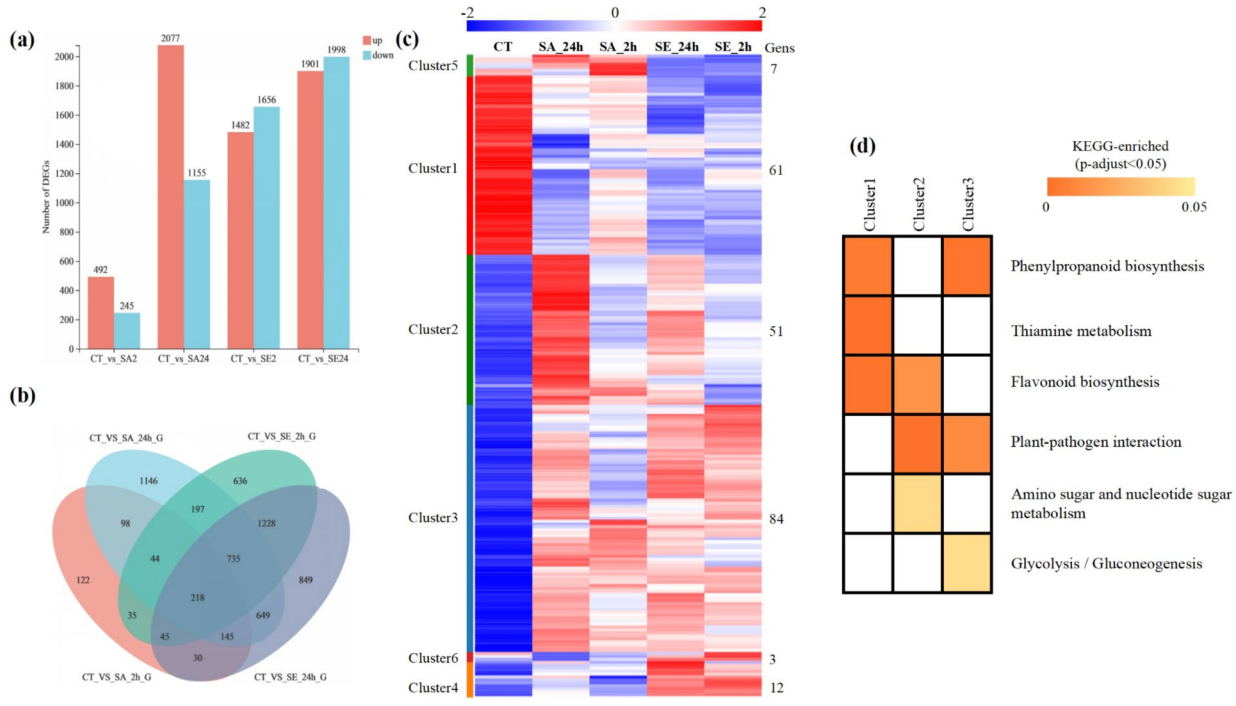

Fig. 1 DEGs in four contrasts. **(a)** Summary of the numbers of DEGs in four contrasts. **(b)** Venn diagram representation of the numbers of DEGs between two contrasts. **(c)** Cluster analysis of common DEGs in four contrasts. **(d)** KEGG pathway analysis of DEGs in the top three clusters. DEGs: Differentially expressed genes; KEGG: Kyoto Encyclopedia of Genes and Genomes

were selected for qRT-PCR. The results showed that two DEGs were upregulated and two DEGs were downregulated, which were consistent with the transcriptome data (Fig. S5).

Metabolites in response to SA and SE stress

In the analysis of the metabolome, a total of 239 DAMs were identified across four groups of samples (SA_12h/CT, SA_24h/CT, SE_12h/CT, and SE_24h/CT). Among all of the DAMs, 46 (12 up and 34 downregulated DAMs) were from SA_12h/CT; 66 (15 up and 51 downregulated DAMs) were from SA_24h/CT; 62 (44 up and 18 downregulated DAMs) were from SE_12h/CT; and 65 (20 up and 45 downregulated DAMs) were from SE_24h/CT (Figs. S6 & S7). The KEGG pathway enrichment analysis indicated that there were significant alterations in two, three, three, and five pathways ($P<0.05$) in SA_12h/CT, SA_24h/CT, SE_12h/CT, and SE_24h/CT, respectively. Furthermore, samples collected at the same time points for SA and SE treatments exhibited two overlapping pathways (Table S4). The primary pathways that demonstrated significant changes following SA and SE treatments included purine metabolism, photosynthesis, ABC transporters, arginine biosynthesis, fructose and mannose metabolism, C5-branched dibasic acid metabolism, glucosinolate biosynthesis, valine, leucine, and isoleucine degradation, as well as cyanoamino acid metabolism (Figs. S8 & S9).

DEGs and DAMs in response to SA and SE stress

The results of KEGG pathway enrichment analysis of DEGs showed that plant hormone signal transduction was important in the responses of *C. equisetifolia* to SA and SE stress. Within the auxin signaling pathway, two genes from the small auxin up RNA (SAUR) family were found to be downregulated, while one gene from the Gretchen Hagen 3 (GH3) family exhibited upregulation in SA_24h/CT, SE_2h/CT, and SE_24h/CT. Additionally, a gene encoding a member of the type-A Arabidopsis response regulator (A-ARR) family, integral to the cytokinin signaling pathway, was downregulated in the groups of SA_24h/CT, SE_2h/CT, and SE_24h/CT. In the ABA signaling pathway, one gene encoding protein phosphatase 2 C (PP2C), one gene encoding sucrose non-fermenting-1-related protein kinase 2 (SnRK2), and another gene encoding ABA-responsive element binding factor (ABF) were upregulated in SA_24h/CT, SE_2h/CT, and SE_24h/CT. Furthermore, there were three upregulated *PP2C* genes in samples with SE treatment. Conversely, genes encoding F-box protein coronatine insensitive 1 (COI1) and myelocytomatosis proteins 2 (MYC2) were downregulated in SE_2h/CT and SE_24h/CT. Notably, one gene encoding the jasmonate ZIM-domain (JAZ) protein showed upregulation across all samples (Fig. 2). Within the plant–pathogen interaction pathway, three genes encoding primary calcium (Ca^{2+}) sensor calmodulin/calmodulin-like (CAM/CML) proteins and two genes encoding pathogenesis related protein 1 (PR1) were upregulated in SA_24h/CT, SE_2h/CT, and SE_24h/CT. Additionally, genes encoding Ca-dependent protein kinases (CDPKs) and TF WRKY33 were upregulated across all samples. Moreover, three genes in the CAM/CML family and two genes in the WRKY 22/29 family were upregulated in SA_24h/CT and SE_24h/CT (Fig. 3).

In the integrated KEGG pathway enrichment analyses of DEGs and DAMs across all samples, key regulatory pathways significantly modified by SA and SE treatments included phenylpropanoid biosynthesis, starch and sucrose metabolism, glycolysis/gluconeogenesis, and amino acid biosynthesis. The phenylpropanoid biosynthesis pathway includes three genes encoding cinnamate 4-hydroxylase (*CYP73A*) and three genes encoding hydroxycinnamoyl transferase (*HCT*) that were upregulated by the SA treatment. The expression levels of two genes encoding cinnamyl alcohol dehydrogenase (*CAD*) were elevated, while the expression level of one gene encoding caffeic acid O-methyltransferase (*COMT*) was downregulated with the SE treatment. Additionally, two genes encoding phenylalanine ammonia lyase (*PALs*) were upregulated, and one gene encoding hydroxycinnamoyl transferase (*HCT*) was downregulated under both SA and SE treatments. Phenylalanine, caffeoyl aldehyde, and sinapyl alcohol concentrations increased in SE_24h/CT, whereas only caffeoyl aldehyde concentration rose in SA_12h/CT. Conversely, caffeoylquinic acid levels decreased in both SA_24h/CT and SE_24h/CT (Fig. 4). In starch and sucrose metabolism, two sucrose synthases (*SUS*s), two invertases (*INV*s), and two terpene synthases (*TPS*s) were found to be upregulated following SE treatment, alongside one downregulated *SUS* and one downregulated *TPS*. In SA_24h/CT, one *SUS*, one *otsB*, and one *INV* were upregulated, while the contents of trehalose-6P and D-glucose were decreased. In glycolysis/gluconeogenesis and biosynthesis of amino acids, 12 h of SA treatment decreased the contents of α-D-glucose-1, $6P_2$, glycerone-P, phosphoenolpyruvate, and 2-oxoglutarate. Additionally, the serine content increased, while the contents of aspartate, methyl aspartate, and ornithine were decreased in SA_24h. After 12 h of SE treatment, both 2-oxoglutarate and methyl aspartate levels decreased (Fig. 5).

Discussion

Effects of SA and SE stress on plant hormone signal transduction

Plant hormones are integral not only to growth and development but also in mediating responses to both biotic and abiotic stress [39, 40]. Phytohormones are

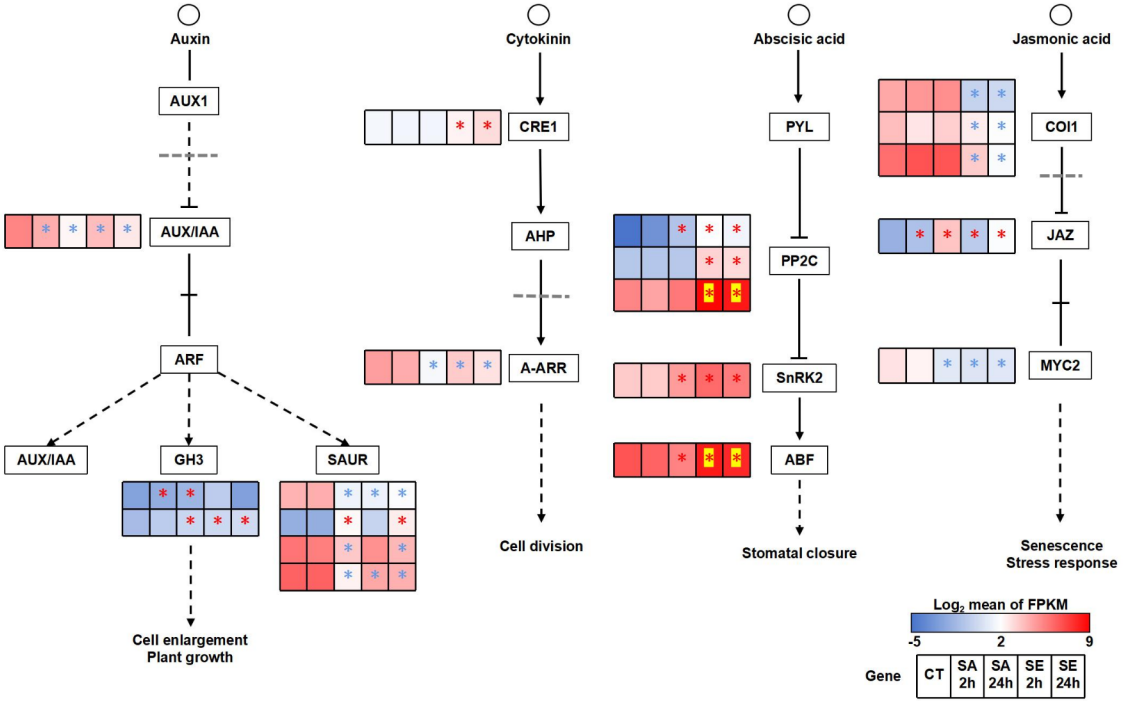

Fig. 2 Genes involved in plant hormone signal transduction in *C. equisetifolia* after exposure to SA and SE stress for 2 and 24 h. The original figure of plant hormone signal transduction pathway was cited from the Kanehisa laboratories [95]. Blue asterisks indicated genes with significantly down-regulated expression and red asterisks indicated genes with significantly up-regulated expression. SA: Seawater atomization; SE: Seawater encroachment; AUX1: Auxin resistant 1; AUX/IAA: Auxin/indole-3-acetic acid; ARF: Auxin response factor; GH3: Gretchen Hagen 3; SAUR: Small auxin-up RNA; CRE1: Cytokinin response 1; AHP: Arabidopsis histidine phosphotransfer proteins; A-ARR: Type-A Arabidopsis response regulator; PYL: Pyrabactin resistance 1-like; PP2C: Protein phosphatase 2 C; Sucrose non-fermenting-1-related protein kinase 2; ABF: ABA-responsive element binding factor; COI1: Coronatine insensitive 1; JAZ: Jasmonate ZIM-domain; MYC2: Myelocytomatosis proteins 2

crucial in stress responses, primarily operating through signal transduction mechanisms [39]. The KEGG enrichment analysis revealed that DEGs were enriched in plant signal transduction pathways following with SA and SE treatments, which were linked to auxin, cytokinin, ABA, and JA signaling pathways. Salt stress results in the accumulation of ABA in plants, which is detected by ABA receptors such as PYR/SnRK2, subsequently influencing the expression of genes involved in the ABA signaling pathway [41]. *PP2C*s encode key enzymes in the ABA signaling pathway. Previous studies have shown that overexpression of *AtPP2CG1* in *Arabidopsis* can improve its salt tolerance [42]. The expression of *ZmPP2C*s was induced by salt stress in *Zea mays* [43], whereas *CsPP2C*s exhibited both increase and decrease in expression levels in *Camellia sinensis* under similar conditions. [44]. SnRK2 proteins have the capacity to phosphorylate ABFs, which play a pivotal role in regulating stomatal closure. [41, 45]. ABA mitigates aqueous depletion by modulating stomatal occlusion, a crucial mechanism for plants experiencing salt stress [2, 46]. In this study, the expression levels of *PP2Cs* and *SnRK2s* were upregulated, suggesting that the ABA signaling pathway is crucial in mediating the response of *C. equisetifolia* to SA and SE stress.

JA is a crucial phytohormone that plays a vital role in the responses of plants to salt stress [47]. In the JA signaling pathway, COI1 engages with JAZ proteins and facilitates their ubiquitination, leading to degradation via the 26 S proteasome pathway. This process releases transcription factors such as MYC2, thereby enhancing the expression of stress responsive genes [47, 48]. JAZ proteins serve as crucial negative regulators within the JA signaling pathway [49]. The genes encoding JAZ in *Ricinus communis* [50], *Arabidopsis* [51], and *Gossypium hirsutum* [52] were found to be upregulated by salt stress. Moreover, overexpression of *MdJAZ2* from apple in *Arabidopsis* improved its drought and salt tolerance [53]. The overexpression of *JAZ9* in rice has been shown to enhance salt tolerance by modulating the expression of the K^+ transporter [54]. In our study, the expression of *JAZ* was enhanced under both SA and SE stress, whereas *MYC2* exhibited downregulation in SA_24h and SE samples. Additionally, we observed that *COI1*s were downregulated only in SE samples. These results indicate that JA signaling pathway was involved in the response of *C. equisetifolia* to SA and SE treatments.

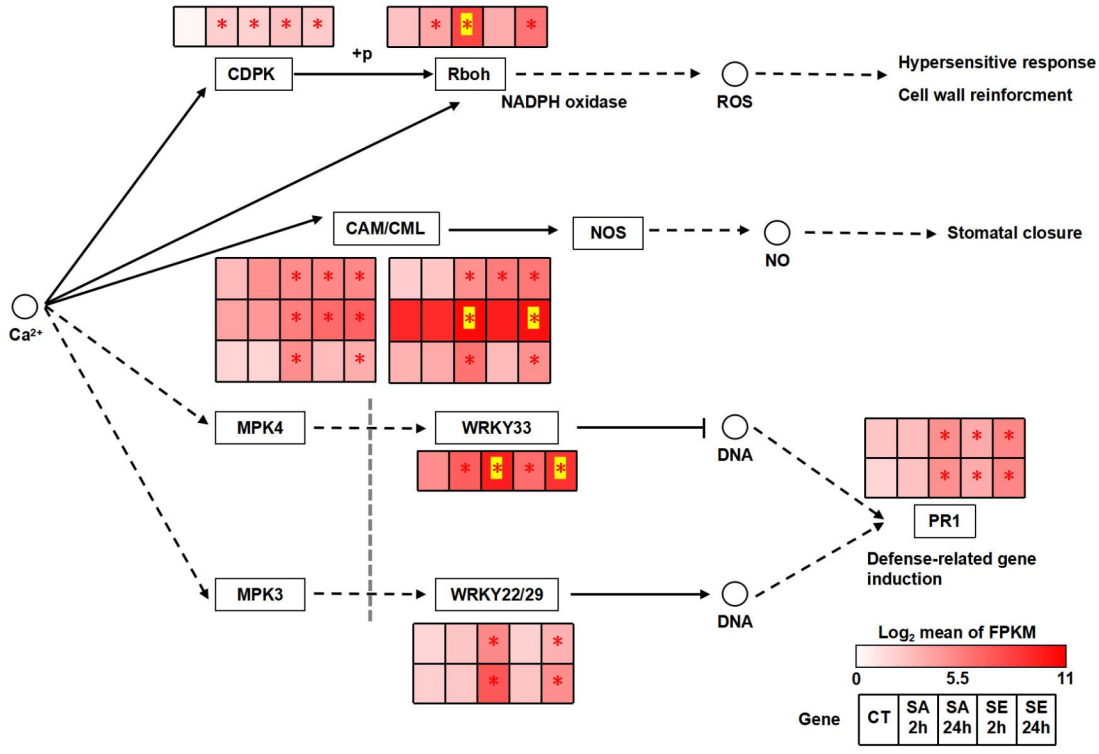

Fig. 3 Genes involved in the plant–pathogen interaction pathway in *C. equisetifolia* after exposure to SA and SE stress for 2 and 24 h. The original figure of plant–pathogen interaction pathway was cited from the Kanehisa laboratories [96, 97]. Red asterisks indicated genes with significantly up-regulated expression. SA: Seawater atomization; SE: Seawater encroachment; CDPK: Calcium-dependent protein kinase; Rboh: Respiratory burst oxidase homolog; CAM/CML: Calmodulin/calmodulin-like proteins; NOS: Nitric oxide synthase; MPK4: Mitogen-activated protein kinase 4; MPK3: Mitogen-activated protein kinase 3; PR1: Pathogenesis related protein-1

Effects of SA and SE stress on the plant–pathogen interaction

In response to saline stress, plant cells exhibit an accumulation of ROS, which serve as signal transducers across multiple signaling pathways, notably those involved in plant–pathogen interactions [55, 56]. In this study, several DEGs were enriched in plant–pathogen interaction pathways in *C. equisetifolia* under SA and SE treatments. *Rboh* genes are responsible for the encoding of NADPH oxidase, a critical enzyme involved in ROS-mediated signaling pathways [57]. Environmental stress leads to changes in Ca^{2+} concentration in plants, which are recognized by specific sensors and then regulated by cascade reactions to regulate the expression of stress-related genes [58, 59]. Notably, CDPK, CAM, and CML proteins serve as crucial Ca^{2+} sensors capable of binding Ca^{2+} through EF-hand motifs [59, 60]. Previous studies have shown that salt stress can activate NADPH oxidase, forming a ROS-Ca^{2+} hub, which is an effective self-amplifying mechanism [61–64]. In this study, the expression of *CDPK* was increased under SA and SE treatments, and the *Rboh* gene was upregulated in SA_2h, SA_24h, and SE_24h samples. The ROS-Ca^{2+} hub possibly participated in the response of *C. equisetifolia* to SA and SE treatments. The WRKY TFs have been identified as playing vital roles in plant responses to abiotic stressors, particularly in relation to salt stress [65, 66]. The *CdWRKY50* was found to be induced by salt stress in *Cynodon dactylon* [67]. Salt stress upregulated the expression of *WRKY86* in maize, subsequently promoting the expression of *Zm00001d020840* and *Zm00001d046813* [68]. The Overexpression of *BcWRKY33* from *B. rapa* in *Arabidopsis* improved the latter's salt tolerance. Moreover, BcWRKY33 interacted with BcHSFA4A odulate gene expression cascades that respond to salt stress [69]. In our study, the expression of *WRKY33* increased under SA and SE treatments, and *WRKY22* and *WRKY29* were upregulated in SA_24h and SE_24h samples. These results suggest that WRKY family genes in *C. equisetifolia* seedlings may activate downstream response transcriptional networks under SA and SE stress.

Effects of SA and SE stress on phenylpropanoid biosynthesis

The phenylpropanoid biosynthesis pathway is vital for plant survival and development. It produces essential precursors, including flavonoids, lignin, and tannin [1, 70]. Studies have shown that phenylpropanoid metabolism positively influences plant responses to salt stress

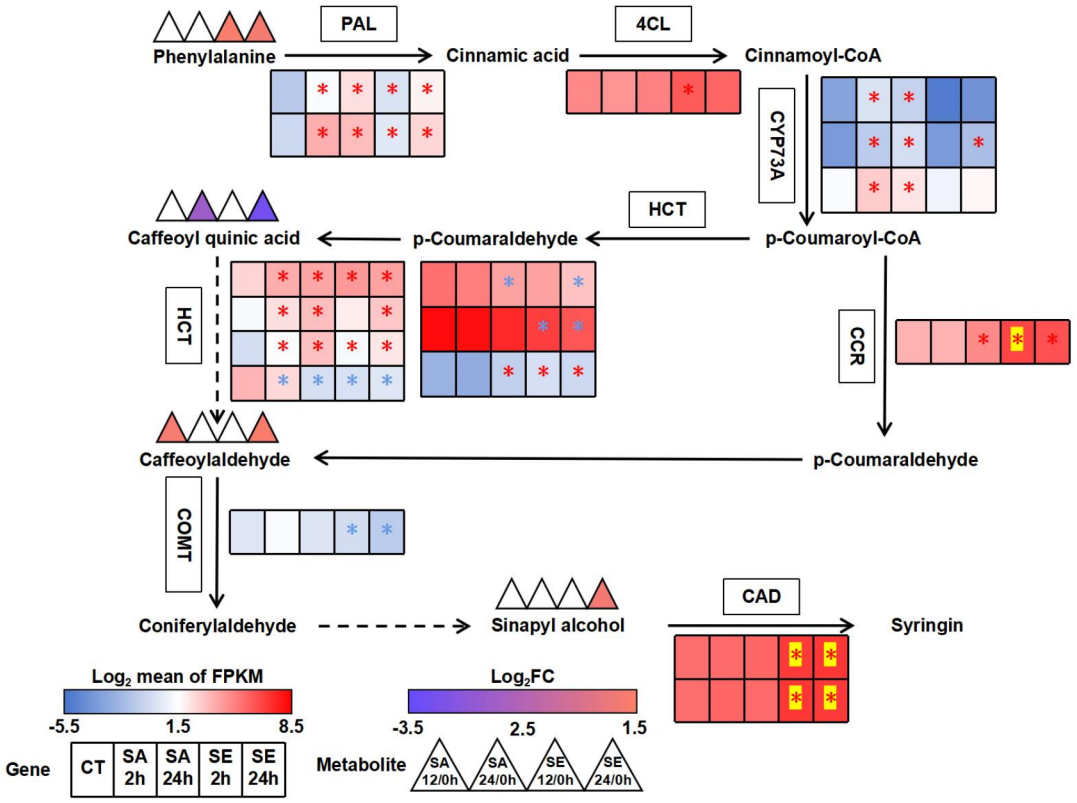

Fig. 4 Genes and DAMs involved in the phenylpropanoid biosynthesis pathway in *C. equisetifolia* after exposure to SA and SE stress for 2 and 24 h for genes, and for 12 and 24 h for metabolites (values are relative to exposure for 0 h). The original figure of phenylpropanoid biosynthesis pathway was cited from the Kanehisa laboratories [96, 97]. Blue asterisks indicated genes with significantly down-regulated expression and red asterisks indicated genes with significantly up-regulated expression. DAMs: Differentially accumulated metabolites; SA: Seawater atomization; SE: Seawater encroachment; PAL: Phenylalanine ammonia lyase; 4CL: 4-coumarate-CoA ligases; CYP73A: Cinnamate 4-hydroxylase; HCT: Hydroxycinnamoyl transferase; CCR: Cinnamoyl-CoA reductase; COMT: Caffeic acid O-methyltransferase; CAD: Cinnamyl alcohol dehydrogenase

[12, 71, 72]. The initial phase of the phenylpropanoid biosynthesis pathway involves two key enzymes: PAL and 4CL. PAL plays a crucial role in modulating the levels of secondary metabolites like flavonoids and lignin when facing environmental stress [1, 73]. Additionally, HCT serves as a vital enzyme, facilitating the transfer of the caffeoyl group back to CoA [1]. Within this metabolic pathway, the enzyme CCR catalyzes the reduction of synthetic caffeoyl aldehyde, while CAD is responsible for synthesizing sinapyl alcohol [74, 75]. In this study, two *PAL*s and two *HCT*s showed increased expression following SA and SE treatments. *CCR* exhibited upregulation in SA_24h and all SE samples. Additionally, two *CAD*s were upregulated across all SE samples. Previous studies indicate that plants accumulate phenolic compounds in response to salt stress. These phenols enhance the plants' antioxidant capacity by effectively scavenging ROS [76, 77]. In our study, the accumulation of caffeoyl aldehyde and sinapyl alcohol increased in SA_12h and SE_24h samples. These results indicate that the phenylpropanoid biosynthesis pathway may play an important role in scavenging ROS in *C. equisetifolia* under SA and SE stress.

Effects of SA and SE stress on primary and secondary metabolism

Soluble sugars play a critical role in plants growth, development, and their responses to environmental stress by mediating sugar signaling pathways [78]. The overexpression of *NINV* in tobacco significantly reduced sucrose content while increased enhancing salt tolerance, suggesting that *NINV* genes can may facilitate plant adaptation to environmental stress through modulation of sugar metabolism [79]. Trehalose protects plant cells from salt, temperature, and drought stress by forming a glassy structure under dehydration conditions [80, 81]. The expression of *TPS*s can enhance the salt tolerance of plants by promoting trehalose biosynthesis [82]. Sucrose acts as a signaling molecule that modulates plant metabolism and triggers stress response mechanisms in plants [83]. SUS can facilitate the reversible transformation of sucrose and UDP into fructose and UDP-glucose [84]. In this study, upregulation of genes encoding INV, SUS, and TPS may contribute to the response of *C. equisetifolia* to SA and SE stress.

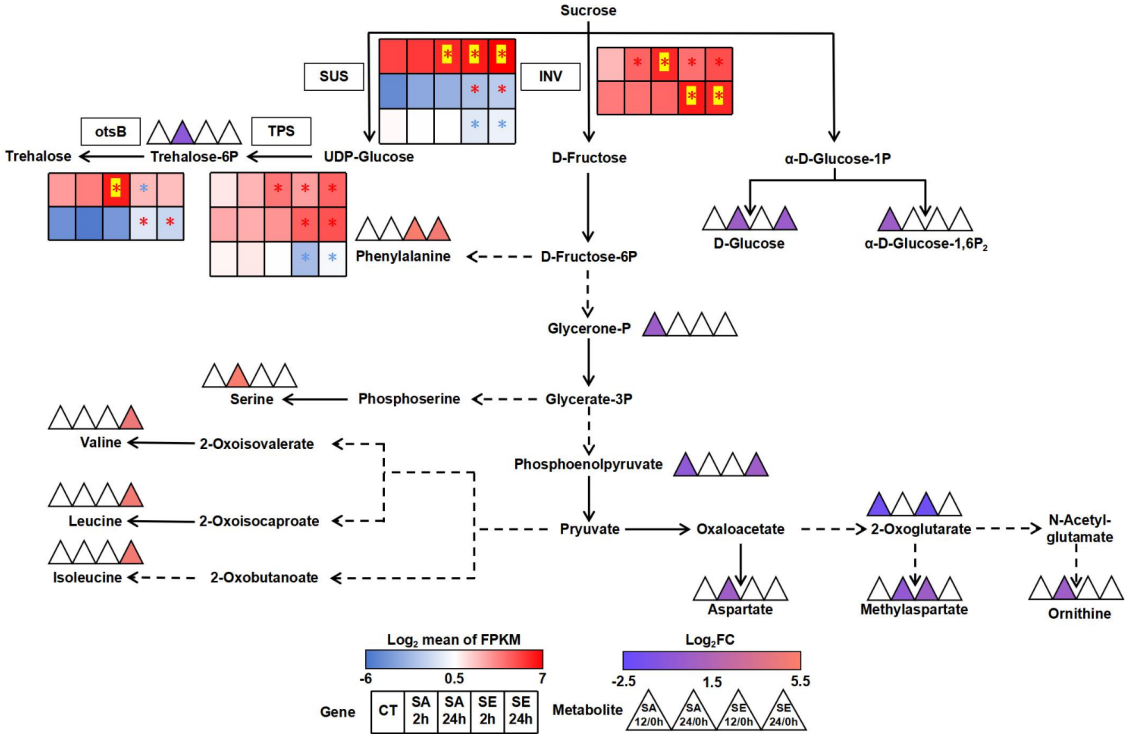

Fig. 5 Genes and DAMs involved in starch and sucrose metabolism, glycolysis/gluconeogenesis, and biosynthesis of amino acids in *C. equisetifolia* after exposure to SA and SE stress for 2 and 24 h for genes, and 12 and 24 h for metabolites (values are relative to exposure for 0 h). The original figure of starch and sucrose metabolism, glycolysis/gluconeogenesis, and biosynthesis of amino acids pathway was cited from the Kanehisa laboratories [96, 97]. Blue asterisks indicated genes with significantly down-regulated expression and red asterisks indicated genes with significantly up-regulated expression DAMs: Differentially accumulated metabolites; SA: Seawater atomization; SE: Seawater encroachment; otsB: Trehalose-6-phosphate phosphatase; TPS: Terpene synthase; SUS: Sucrose synthase; INV: Invertase

Respiration supplies the energy and carbon essential for plant growth and development [85]. Glycolysis plays a crucial role in this process by generating ATP under anaerobic conditions and offering precursors for the biosynthesis of proteins, sugars, and lipids [86]. In this study, the content of glycerone-P and phosphoenolpyruvate decreased in SA_12h sample, which may provide energy for the response of *C. equisetifolia* to SA stress. In addition to functioning as the fundamental building blocks of proteins, amino acids can also serve as osmotic regulators, enhancing plant resilience to osmotic stress [10]. The contents of valine, leucine, and isoleucine increased in the SE_24h sample, indicating that these amino acids may help maintain the osmotic pressure of *C. equisetifolia* under SE treatment. Taken together, these results indicated that starch and sucrose metabolism, glycolysis/gluconeogenesis, and amino acid biosynthesis were important in the response of *C. equisetifolia* to SA and SE treatments.

Differences in response of *C. equisetifolia* to SA and SE stress

The plant hormone signal transduction pathway is crucial in stress perception and response [87]. In this study, we found that the number of DEGs in the plant hormone signal transduction pathway under SA stress was lower than that under SE stress, and these DEGs were mainly concentrated in the later stage of SA treatment (24 h). Since SE treatment involves flooding and salinity stress, *C. equisetifolia* may perceive it more strongly. Previous studies have shown that plants respond to flooding by regulating the expression of genes in hormone signaling, phenylpropanoid, amino acid and primary sugars biosynthesis [88, 89]. The SA treatment was achieved by directly applying salt spray to the aboveground parts of *C. equisetifolia*. In the early stage of SA treatment (2 h), only a few genes showed significant changes in expression, which may be due to the alleviation of stress response by the morphological structure of branchlets [90]. Furthermore, the salinity stress induced by SA treatment is likely to be less intense than the combined effects of flooding and salinity stress from SE treatment, which accounts for the number of DEGs in SA_24h were less compared to those in SE_24h.

In the plant–pathogen interaction pathway, the CAM/CML family participates in the regulation of stomatal closure process [91]. In this study, six DEGs belonging to the CAM/CML family were identified in SA_24h, SE_2h,

and SE_24h. Different from SA treatment, the expression of three DEGs was significantly upregulated in the entire stage of SE treatment (2 and 24 h). It was found that seawater flooding reduced the stomatal conductance of *Phoenix dactylifera* [92]. In this study, the extent of stomatal closure induced by SE treatment may exceed that of SA treatment. Previous studies have shown that salt stress alters *PR1* expression by inducing ROS accumulation [93]. Compared with SA treatment, the expression of *PR1*s was significantly upregulated in the entire stage of SE treatment (2 and 24 h), which might be due to the additive effects of flooding and salinity.

The phenylpropanoid biosynthesis pathway is vital in plant response to salt stress [12, 71, 72]. We found that there were more DEGs in the phenylpropanoid biosynthesis pathway under SE treatment, which may indicate that *C. equisetifolia* was subjected to more severe oxidative stress. Moreover, we found that DAMs were mainly concentrated in the late stage of SE treatment (24 h), which indicated that *C. equisetifolia* may clear excess ROS by accumulating phenolic compounds.

The starch and sucrose metabolism can provide energy and carbon storage for plants under stress [94]. The DEGs in starch and sucrose metabolism were mainly concentrated in the late stage of SA treatment (24 h) and the entire stage of SE treatment (2 and 24 h). It may be that *C. equisetifolia* requires more energy to cope with SE stress. The accumulation of amino acids helps plants adapt to osmotic stress [2, 4]. We found that various amino acids (valine, leucine, isoleucine, and phenylalanine) accumulated in SE_24h, which may be a strategy for *C. equisetifolia* to cope with osmotic stress caused by SE treatment.

Conclusion

In this study, the transcript and metabolic profiles were analyzed to reveal the mechanisms underlying *C. equisetifolia*'s response to SA and SE stress. The KEGG enrichment analysis showed that SA and SE stress significantly changed the expression of genes involved in plant hormone signal transduction, plant–pathogen interaction, and starch and sucrose metabolism pathways. Our results also showed that SA and SE stress increased the accumulation of amino acids and phenolic compounds, such as serine, valine, and caffeoyl aldehyde, which could help *C. equisetifolia* cope with osmotic and oxidative stress. Compared with SA stress, *C. equisetifolia* had a stronger perception and response to SE stress, which required more genes and metabolites to be regulated. These results increase our understanding how *C. equisetifolia* responds to SA and SE stress at transcriptional and metabolic levels and offer a theoretical framework for effective coastal vegetation management.

Supplementary Information

The online version contains supplementary material available at https://doi.org/10.1186/s12870-024-05561-z.

Supplementary Material 1

Acknowledgements
We thank Kanehisa Laboratories for copyright permission of KEGG and Dr. Yuheng Zhou for technical assistance.

Author contributions
N. L., S. J., and S. Z. conceived and designed the project. S. Z., N. L., and S. J. analyzed the data and wrote the manuscript. N. L., S. J., L. W., G. W., W. Y., C. G., D. L., L. G., and J. Y. supervised and revised the manuscript. All authors read and approved the manuscript.

Funding
This study was supported the National Key R&D Program of China (2021YFC3100401, 2022YFC3103700), the High-level Talent Research Start-up Project Funding of Henan Academy of Sciences (Project NO. 241801041, Project NO. 231801034), the Science and Technology Research Project of Henan Province (242102320323), the Joint Fund of Henan Province Science and Technology R&D Program (Project NO. 225200810104), the Forestry Science and Technology Innovation Fund Project of Guangdong Province (2021KYXM09, 2022KYXM09, 2022KJCX005), Natural Science Foundation of Guangdong Province (2021A1515011670), and Guangdong Science and Technology Plan Project (Grant No. 2023B1212060046).

Data availability
The sequenced raw reads generated in this study have been submitted to NCBI w-ith BioProject ID: PRJNA983994 (https://dataview.ncbi.nlm.nih.gov/object/PRJNA983994?reviewer=9l7862c0ce35e9ad0jrtt8t87b).

Declarations

Ethics approval and consent to participate
The *C. equisetifolia* ssp. *incana* seedlings were collected from South China Botanical Garden and were identified by professor Shuguang Jian and Nan Liu. The methods involved in this study were carried out in compliance with local and national regulations.

Consent for publication
Not applicable.

Competing interests
The authors declare no competing interests.

Received: 30 May 2024 / Accepted: 2 September 2024
Published online: 12 September 2024

References

1. Dong N, Lin H. Contribution of phenylpropanoid metabolism to plant development and plant-environment interactions. J Integr Plant Biol. 2021;63:180–209.
2. Patel M, Parida A. Salinity mediated cross-tolerance of arsenic toxicity in the halophyte *Salvadora Persica* L. through metabolomic dynamics and regulation of stomatal movement and photosynthesis. Environ Pollut. 2022;300:118888.
3. Shelden M, Dias D, Jayasinghe N, Bacic A, Roessner U. Root spatial metabolite profiling of two genotypes of barley (*Hordeum vulgare* L.) reveals differences in response to short-term salt stress. J Exp Bot. 2016;67:3731–45.
4. Cao B, Li N, Xu K. Crosstalk of phenylpropanoid biosynthesis with hormone signaling in Chinese cabbage is key to counteracting salt stress. Environ Exp Bot. 2020;179:104209.
5. Wang Y, Zhang Y, Fan C, Wei Y, Meng J, Li Z, Zhong C. Genome-wide analysis of MYB transcription factors and their responses to salt stress in *Casuarina equisetifolia*. BMC Plant Biol. 2021;21:328.

6. Du J, Hesp A. Salt spray distribution and its impact on vegetation zonation on coastal dunes: a review. Estuar Coast. 2020;43:1885–907.
7. Hayes M, Chapman S, Jesse A, O'Brien E, Langley J, Bardou R, Devaney J, Parker J, Cavanaugh K. Foliar water uptake by coastal wetland plants: a novel water acquisition mechanism in arid and humid subtropical mangroves. J Ecol. 2020;108:2625–37.
8. Sun X, Li D, Chen H, Ma Z, Xiao K, Yan J, Wang Z, Duan P. Divergent responses of symbiotic and asymbiotic N_2 fixation to seawater additions. Funct Ecol. 2021;35:2789–98.
9. Wang F, Ge S, Xu X, Xing Y, Du X, Zhang X, Lv M, Liu J, Zhu Z, Jiang Y. Multiomics analysis reveals new insights into the apple fruit quality decline under high nitrogen conditions. J Agric Food Chem. 2021;69:5559–72.
10. Derakhshani Z, Bhave M, Shah RM. Metabolic contribution to salinity stress response in grains of two barley cultivars with contrasting salt tolerance. Environ Exp Bot. 2020;179:104229.
11. Shen Z, Chen J, Ghoto K, Hu W, Gao G, Luo M, Li Z, Simon M, Zhu X, Zheng H. Proteomic analysis on mangrove plant *Avicennia marina* leaves reveals nitric oxide enhances the salt tolerance by up-regulating photosynthetic and energy metabolic protein expression. Tree Physiol. 2018;38:1605–22.
12. Wang L, Pan D, Lv X, Cheng C, Li J, Liang W, Xing J, Chen W. A multilevel investigation to discover why *Kandelia Candel* thrives in high salinity. Plant Cell Environ. 2016;39:2486–97.
13. Thalmann M, Santelia D. Starch as a determinant of plant fitness under abiotic stress. New Phytol. 2017;214:943–51.
14. Wang X, Chang L, Wang B, Wang D, Li P, Wang L, Yi X, Huang Q, Peng M, Guo A. Comparative proteomics of *Thellungiella halophila* leaves from plants subjected to salinity reveals the importance of chloroplastic starch and soluble sugars in halophyte salt tolerance. Mol Cell Proteom. 2013;12:2174–95.
15. Nakabayashi R, Yonekura-Sakakibara K, Urano K, Suzuki M, Yamada Y, Nishizawa T, Matsuda F, Kojima M, Sakakibara H, Shinozaki K, et al. Enhancement of oxidative and drought tolerance in *Arabidopsis* by overaccumulation of antioxidant flavonoids. Plant J. 2014;77:367–79.
16. Zhang D, Li J, Niu X, Deng C, Song X, Li W, Cheng Z, Xu Q, Zhang B, Guo W. GhANN1 modulates the salinity tolerance by regulating ABA biosynthesis, ion homeostasis and phenylpropanoid pathway in cotton. Environ Exp Bot. 2021;185:104427.
17. Devireddy A, Zandalinas S, Fichman Y, Mittler R. Integration of reactive oxygen species and hormone signaling during abiotic stress. Plant J. 2021;105:459–76.
18. Zhu J. Abiotic stress signaling and responses in plants. Cell. 2016;167:313–24.
19. Dinneny J. Traversing organizational scales in plant salt-stress responses. Curr Opin Plant Biol. 2015;23:70–5.
20. Zhu J. Salt and drought stress signal transduction in plants. Annu Rev Plant Biol. 2002;53:247–73.
21. Pan J, Li Z, Wang Q, Guan Y, Li X, Huangfu Y, Meng F, Li J, Dai S, Liu W. Phosphoproteomic profiling reveals early salt-responsive mechanisms in two Foxtail millet cultivars. Front. Plant Sci. 2021;12:712257.
22. Julkowska M, Testerink C. Tuning plant signaling and growth to survive salt. Trends Plant Sci. 2015;20:586–94.
23. Jammes F, Song C, Shin D, Munemasa S, Takeda K, Gu D, Cho D, Lee S, Giordo R, Sritubtim S, et al. MAP kinases *MPK9* and *MPK12* are preferentially expressed in guard cells and positively regulate ROS-mediated ABA signaling. Proc Natl Acad Sci USA. 2009;106:20520–5.
24. Fan C, Qiu Z, Zeng B, Li X, Xu SH. Physiological adaptation and gene expression analysis of *Casuarina equisetifolia* under salt stress. Biol Plant. 2018;62:489–500.
25. Fan C, Qiu Z, Zeng B, Liu Y, Li X, Guo G. Selection of reference genes for quantitative real-time PCR in *Casuarina equisetifolia* under salt stress. Biol Plant. 2017;61:463–72.
26. Selvakesavan R, Dhanya N, Thushara P, Abraham S, Jayaraj R, Balasubramanian A, Deeparaj B, Sudha S, Rani KS, Bachpai V, et al. Intraspecies variation in sodium partitioning, potassium and proline accumulation under salt stress in *Casuarina equisetifolia* Forst. Symbiosis. 2016;70:117–27.
27. Tani C, Sasakawa H. Proline accumulates in *Casuarina equisetifolia* seedlings under salt stress. Soil Sci Plant Nutr. 2006;52:21–5.
28. Wang Y, Zhang J, Qiu Z, Zeng B, Zhang Y, Wang X, Chen J, Zhong C, Deng R, Fan C. Transcriptome and structure analysis in root of *Casuarina equisetifolia* under NaCl treatment. PEERJ. 2021;9:e12133.
29. Nie B, Chen T, Liang M, Wang Y, Zhong J, Zhu Y. Relationship between coral growth rate and sea surface temperature in the northern part of South China Sea during the past 100 a. Sci China Ser D. 1997;40:173–82.
30. Ye G, Zhang H, Chen B, Nie S, Liu H, Gao W, Wang H, Gao Y, Gu L. *De novo* genome assembly of the stress tolerant forest species *Casuarina equisetifolia* provides insight into secondary growth. Plant J. 2019;97:779–94.
31. Kim D, Langmead B, Salzberg S. HISAT: a fast spliced aligner with low memory requirements. Nat Methods. 2015;12:357–U121.
32. Li B, Dewey C. RSEM: accurate transcript quantification from RNA-Seq data with or without a reference genome. BMC Bioinform. 2011;12:323.
33. Love M, Huber W, Anders S. Moderated estimation of Fold change and dispersion for RNA-seq data with DESeq2. Genome Biol. 2014;15:550.
34. Xie C, Mao X, Huang J, Ding Y, Wu J, Dong S, Kong L, Gao G, Li C-Y, Wei L. KOBAS 2.0: a web server for annotation and identification of enriched pathways and diseases. Nucleic Acids Res. 2011;39:W316–22.
35. Guo H, Guo H, Zhang L, Tang Z, Yu X, Wu J, Zeng F. Metabolome and transcriptome association analysis reveals dynamic regulation of purine metabolism and flavonoid synthesis in transdifferentiation during somatic embryogenesis in cotton. Int J Mol Sci. 2019;20:2070.
36. Si C, Zeng D, Yu Z, da Silva J, Duan J, He C, Zhang J. Transcriptomic and metabolomic analyses reveal the main metabolites in *Dendrobium officinale* leaves during the harvesting period. Plant Physiol Biochem. 2022;190:24–34.
37. Veluthakkal R, Dasgupta M. Isolation and characterization of pathogen defence-related class I chitinase from the actinorhizal tree *Casuarina equisetifolia*. Pathol. 2012;42:467–80.
38. Livak K, Schmittgen T. Analysis of relative gene expression data using real-time quantitative PCR and the $2^{-\Delta\Delta C}_{T}$ method. Methods. 2001;25:402–8.
39. Yu Z, Duan X, Luo L, Dai S, Ding Z, Xia G. How plant hormones mediate salt stress responses. Trends Plant Sci. 2020;25:1117–30.
40. Wei T, Wang Y, Liu J. Comparative transcriptome analysis reveals synergistic and disparate defense pathways in the leaves and roots of trifoliate orange (*Poncirus trifoliata*) autotetraploids with enhanced salt tolerance. Hortic Res. 2020;7:88.
41. Zhao Y, Chan Z, Gao J, Xing L, Cao M, Yu C, Hu Y, You J, Shi H, Zhu Y, et al. ABA receptor PYL9 promotes drought resistance and leaf senescence. Proc Natl Acad Sci USA. 2016;113:1949–54.
42. Liu X, Zhu Y, Zhai H, Cai H, Ji W, Luo X, Li J, Bai X. AtPP2CG1, a protein phosphatase 2 C, positively regulates salt tolerance of *Arabidopsis* in abscisic acid-dependent manner. Biochem Biophys Res Commun. 2012;422:710–5.
43. Tan M. Analysis of DNA methylation of maize in response to osmotic and salt stress based on methylation-sensitive amplified polymorphism. Plant Physiol Biochem. 2010;48:21–6.
44. Wan S, Wang W, Zhou T, Zhang Y, Chen J, Xiao B, Yang Y, Yu Y. Transcriptomic analysis reveals the molecular mechanisms of *Camellia sinensis* in response to salt stress. Plant Growth Regul. 2018;84:481–92.
45. Cai S, Chen G, Wang Y, Huang Y, Marchant D, Wang Y, Yang Q, Dai F, Hills A, Franks P, et al. Evolutionary conservation of ABA signaling for stomatal closure. Plant Physiol. 2017;174:732–47.
46. Gong Z, Xiong L, Shi H, Yang S, Herrera-Estrella L, Xu G, Chao D, Li J, Wang P, Qin F, et al. Plant abiotic stress response and nutrient use efficiency. Sci China-Life Sci. 2020;63:635–74.
47. Wasternack C, Song S. Jasmonates: biosynthesis, metabolism, and signaling by proteins activating and repressing transcription. J Exp Bot. 2017;68:1303–21.
48. Wasternack C, Hause B. Jasmonates: biosynthesis, perception, signal transduction and action in plant stress response, growth and development. Ann Bot. 2013;111:1021–58.
49. Monte I, Franco-Zorrilla J, Garcia-Casado G, Zamarreno A, Garcia-Mina J, Nishihama R, Kohchi T, Solano R. A single JAZ repressor controls the jasmonate pathway in *Marchantia polymorpha*. Mol Plant. 2019;12:185–98.
50. Lei P, Liu Z, Hu Y, Kim H, Liu S, Liu J, Xu L, Li J, Zhao Y, Yu Z, et al. Transcriptome analysis of salt stress responsiveness in the seedlings of wild and cultivated *Ricinus communis* L. J Biotechnol. 2021;327:106–16.
51. Valenzuela C, Acevedo-Acevedo O, Miranda G, Vergara-Barros P, Holuigue L, Figueroa C, Figueroa P. Salt stress response triggers activation of the jasmonate signaling pathway leading to inhibition of cell elongation in *Arabidopsis* primary root. J Exp Bot. 2016;67:4209–20.
52. Yao D, Zhang X, Zhao X, Liu C, Wang C, Zhang Z, Zhang C, Wei Q, Wang Q, Yan H, et al. Transcriptome analysis reveals salt-stress-regulated biological processes and key pathways in roots of cotton (*Gossypium hirsutum* L). Genomics. 2011;98:47–55.
53. An X, Hao Y, Li E, Xu K, Cheng C. Functional identification of apple *MdJAZ2* in *Arabidopsis* with reduced JA-sensitivity and increased stress tolerance. Plant Cell Rep. 2017;36(2):255–65.

54. Wu H, Ye H, Yao R, Zhang T, Xiong L. *OsJAZ9* acts as a transcriptional regulator in jasmonate signaling and modulates salt stress tolerance in rice. Plant Sci. 2015;232:1–12.
55. Camejo D, Guzman-Cedeno A, Moreno A. Reactive oxygen species, essential molecules, during plant-pathogen interactions. Plant Physiol Biochem. 2016;103:10–23.
56. Miller E, Dickinson B, Chang C. Aquaporin-3 mediates hydrogen peroxide uptake to regulate downstream intracellular signaling. Proc Natl Acad Sci USA. 2010;107:15681–6.
57. Liu M, Yu H, Ouyang B, Shi C, Demidchik V, Hao Z, Yu M, Shabala S. NADPH oxidases and the evolution of plant salinity tolerance. Plant Cell Environ. 2020;43:2957–68.
58. McAinsh M, Pittman J. Shaping the calcium signature. New Phytol. 2009;181:275–94.
59. Singh A, Sagar S, Biswas D. Calcium dependent protein kinase, a versatile player in plant stress management and development. Crit Rev Plant Sci. 2017;36:336–52.
60. Zhang X, Wang T, Liu M, Sun W, Zhang W. Calmodulin-like gene *MtCML40* is involved in salt tolerance by regulating MtHKTs transporters in *Medicago truncatula*. Environ Exp Bot. 2019;157:79–90.
61. Chung J, Zhu J, Bressan R, Hasegawa P, Shi H. Reactive oxygen species mediate Na^+-induced *SOS1* mRNA stability in *Arabidopsis*. Plant J. 2008;55:554–65.
62. Marino D, Dunand C, Puppo A, Pauly N. A burst of plant NADPH oxidases. Trends Plant Sci. 2012;17:9–15.
63. Demidchik V, Shabala S, Isayenkov S, Cuin T, Pottosin I. Calcium transport across plant membranes: mechanisms and functions. New Phytol. 2018;220:49–69.
64. Foreman J, Demidchik V, Bothwell J, Mylona P, Miedema H, Torres M, Linstead P, Costa S, Brownlee C, Jones J, et al. Reactive oxygen species produced by NADPH oxidase regulate plant cell growth. Nature. 2003;422:442–6.
65. Zhou Q, Tian A, Zou H, Xie Z, Lei G, Huang J, Wang C, Wang H, Zhang J, Chen S. Soybean WRKY-type transcription factor genes, GmWRKY13, GmWRKY21, and GmWRKY54, confer differential tolerance to abiotic stresses in transgenic Arabidopsis plants. Plant Biotechnol J. 2008;6:486–503.
66. Dai W, Wang M, Gong X, Liu J. The transcription factor FcWRKY40 of *Fortunella crassifolia* functions positively in salt tolerance through modulation of ion homeostasis and proline biosynthesis by directly regulating *SOS2* and *P5CS1* homologs. New Phytol. 2018; 219: 972–989.
67. Huang X, Amee M, Chen L. Bermudagrass *CdWRKY50* gene negatively regulates plants' response to salt stress. Environ Exp Bot. 2021;188:104513.
68. Fang X, Li W, Yuan H, Chen H, Bo C, Ma Q, Cai R. Mutation of *ZmWRKY86* confers enhanced salt stress tolerance in maize. Plant Physiol Biochem. 2021;167:840–50.
69. Wang H, Li Z, Ren H, Zhang C, Xiao D, Li Y, Hou X, Liu T. Regulatory interaction of BcWRKY33A and BcHSFA4A promotes salt tolerance in non-heading Chinese cabbage *Brassica campestris* (syn. *Brassica rapa*) ssp. *chinensis*. Hortic Res. 2022;9:uhac113.
70. Gray J, Caparros-Ruiz D, Grotewold E. Grass phenylpropanoids: regulate before using! Plant Sci. 2012;184:112–20.
71. Amarasinghe S, Watson-Haigh N, Byrt C, James R, Qiu J, Berkowitz O, Whelan J, Roy S, Gilliham M, Baumann U. Transcriptional variation is associated with differences in shoot sodium accumulation in distinct barley varieties. Environ Exp Bot. 2019;166:103812.
72. Crizel R, Perin E, Siebeneichler T, Borowski J, Messias R, Rombaldi C, Galli V. Abscisic acid and stress induced by salt: Effect on the phenylpropanoid, L-ascorbic acid and abscisic acid metabolism of strawberry fruits. Plant Physiol Biochem. 2020;152:211–20.
73. Li G, Wang H, Cheng X, Su X, Zhao Y, Jiang T, Jin Q, Lin Y, Cai Y. Comparative genomic analysis of the *PAL* genes in five Rosaceae species and functional identification of Chinese white pear. PEERJ. 2019;7:e8064.
74. Lacombe E, Hawkins S, VanDoorsselaere J, Piquemal J, Goffner D, Poeydomenge O, Boudet AM, GrimaPettenati J. Cinnamoyl CoA reductase, the first committed enzyme of the lignin branch biosynthetic pathway: Cloning, expression and phylogenetic relationships. Plant J. 1997;11(3):429–41.
75. Barros J, Escamilla-Trevino L, Song L, Rao X, Serrani-Yarce J, Palacios M, Engle N, Choudhury F, Tschaplinski T, Venables B, et al. 4-Coumarate 3-hydroxylase in the lignin biosynthesis pathway is a cytosolic ascorbate peroxidase. Nat Commun. 2019;10:1994.
76. Yan K, Bian L, He W, Han G, Zhang Z, Sun Z, Liang L, Jia H, Wang G. Phytohormone signaling pathway for eliciting leaf phenolic synthesis in honeysuckle (*Lonicera japonica* Thunb.) Under coastal saline environment. Ind Crops Prod. 2020;157:112929.
77. Cheynier V, Comte G, Davies K, Lattanzio V, Martens S. Plant phenolics: recent advances on their biosynthesis, genetics, and ecophysiology. Plant Physiol Bioch. 2013;72:1–20.
78. Ruan Y, Jin Y, Yang Y, Li G, Boyer J. Sugar input, metabolism, and signaling mediated by invertase: roles in development, yield potential, and response to drought and heat. Mol Plant. 2010;3:942–55.
79. Dahro B, Wang F, Peng T, Liu J. PtrA/NINV, an alkaline/neutral invertase gene of Poncirus trifoliata, confers enhanced tolerance to multiple abiotic stresses by modulating ROS levels and maintaining photosynthetic efficiency. BMC Plant Biol. 2016;16:76.
80. Goddijn O, van Dun K. Trehalose metabolism in plants. Trends Plant Sci. 1999;4:315–9.
81. Garg A, Kim J, Owens T, Ranwala A, Do Choi Y, Kochian L, Wu R. Trehalose accumulation in rice plants confers high tolerance levels to different abiotic stresses. Proc Natl Acad Sci USA. 2002;99:15898–903.
82. Qin L, Wang L, Guo Y, Li Y, Umut H, Wang Y. An ERF transcription factor from *Tamarix Hispida*, ThCRF1, can adjust osmotic potential and reactive oxygen species scavenging capability to improve salt tolerance. Plant Sci. 2017;265:154–66.
83. Ruan Y. Sucrose metabolism: gateway to diverse carbon use and sugar signaling. Annu Rev Plant Biol. 2014;65:33–67.
84. Huang Y, Hsiang E, Yang C, Wang A. New insight into the catalytic properties of rice sucrose synthase. Plant Mol Biol. 2016;90:127–35.
85. O'Leary B, Asao S, Millar A, Atkin O. Core principles which explain variation in respiration across biological scales. New Phytol. 2019;222:670–86.
86. Zhao X, Chen Z, Leng P, Hu Z. iTRAQ-based quantitative proteomic analysis of the response of *Hylotelephium erythrostictum* leaves to salt stress. Sci Hortic. 2020;264:109190.
87. Shan X, Yan J, Xie D. Comparison of phytohormone signaling mechanisms. Curr Opin Plant Biol. 2012;15:84–91.
88. Wang F, Zhou Z, Liu X, Zhu L, Guo B, Lv C, Zhu J, Chen Z, Xu R. Transcriptome and metabolome analyses reveal molecular insights into waterlogging tolerance in Barley. BMC Plant Biol. 2024;24:385.
89. Ateeq M, Khan A, Zhang D, Alam S, Shen W, Wei M, Meng J, Shen X, Pan J, Zhu K, He H, Li G, Liu J. Comprehensive physio-biochemical and transcriptomic characterization to decipher the network of key genes under waterlogging stress and its recuperation in. Prunus persica Tree Physiol. 2023;43:1265–83.
90. Dörken V, Parsons R. Morpho-anatomical studies on the leaf reduction in Casuarina: the ecology of xeromorphy. Trees-struct Funct. 2017;31:1165–77.
91. Delormel T, Boudsocq M. Properties and functions of calcium-dependent protein kinases and their relatives in Arabidopsis thaliana. New Phytol. 2019;224:585–604.
92. Du B, Ma Y, Yáñez A, Arab L, Fasbender L, Alfarraj S, Albasher G, Hedrich R, White P, Werner C, Rennenberg H. Physiological responses of date palm (*Phoenix dactylifera*) seedlings to seawater and flooding. New Phytol. 2021;229:3318–29.
93. Chojak-Kozniewska J, Linkiewicz A, Sowa S, Radzioch M, Kuzniak E. Interactive effects of salt stress and *Pseudomonas syringae* Pv. *Lachrymans* infection in cucumber: involvement of antioxidant enzymes, abscisic acid and salicylic acid. Environ Exp Bot. 2017;136:9–20.
94. Zhou H, Liu M, Meng F, Zheng D, Feng N. Transcriptomics and physiology reveal the mechanism of potassium indole-3-butyrate (IBAK) mediating rice resistance to salt stress. BMC Plant Biol. 2023;23:569.
95. Kanehisa M, Goto S. KEGG: Kyoto Encyclopedia of genes and genomes. Nucleic Acids Res. 2000;28:27–30.
96. Kanehisa M. Toward understanding the origin and evolution of cellular organisms. Protein Sci. 2019;28:1947–51.
97. Kanehisa M, Furumichi M, Sato Y, Kawashima M, Ishiguro-Watanabe M. KEGG for taxonomy-based analysis of pathways and genomes. Nucleic Acids Res. 2023;51:D587–92.

Publisher's note